minerals

MDPI

Article

Oily Bubble Flotation of Coal Macerals of Shendong Jurassic Coal

Jinzhou Qu [1,2,*], Chang Luo [1], Zhanglei Zhu [1,2], Quan An [3], Xinyi Li [1], Honglin Zhu [1], Jing Chang [1,2], Zhen Li [1,2], Anning Zhou [1,2], Songjiang Chen [1,2] and Ningning Zhang [1,2]

[1] College of Chemistry and Chemical Engineering, Xi'an University of Science and Technology, Xi'an 710054, China
[2] Key Laboratory of Coal Resources Exploration and Comprehensive Utilization, Ministry of Natural Resources, Xi'an 710021, China
[3] Shaanxi Boxuan Technology Co., Ltd., Xi'an 710026, China
* Correspondence: qujinzhou@xust.edu.cn

Abstract: The comprehensive quality enhancement and grading of coal are crucial methods for unlocking the high value-added and low-carbon utilization of coal resources. In this work, the influence of oily bubbles on the flotation of Shendong Jurassic vitrinite-rich coal and inertinite-rich coal was studied via flotation tests, Fourier transform infrared (FT-IR) spectroscopy, X-ray photoelectron spectroscopy (XPS), contact angle detection, and induction time measurements. FT-IR and XPS analyses demonstrated that the surface of inertinite-rich coal contains more hydrophilic oxygen-containing functional groups. Contact angle and induction time measurements showed that the vitrinite-rich coal is more hydrophobic than inertinite-rich coal, and that for both air and oily bubbles, the induction time on the surface of vitrinite-rich coal is shorter than that on the surface of inertinite-rich coal. In addition, rather remarkably, the induction times for both vitrinite-rich coal and inertinite-rich coal are significantly reduced by oily bubbles. Finally, a better flotation performance for oily bubble flotation of vitrinite-rich coal and inertinite-rich coal was found. It appears that oily bubble flotation is an efficient method for enhancing the recovery of vitrinite-rich coal and inertinite-rich coal.

Keywords: vitrinite-rich coal; inertinite-rich coal; oily bubble; induction time; functional groups; wettability

Citation: Qu, J.; Luo, C.; Zhu, Z.; An, Q.; Li, X.; Zhu, H.; Chang, J.; Li, Z.; Zhou, A.; Chen, S.; et al. Oily Bubble Flotation of Coal Macerals of Shendong Jurassic Coal. *Minerals* **2024**, *14*, 328. https://doi.org/10.3390/min14040328

Academic Editor: M. Thaddeus Ityokumbul

Received: 25 December 2023
Revised: 10 March 2024
Accepted: 20 March 2024
Published: 22 March 2024

1. Introduction

Differentiated upgrading and classification of coal are essential prerequisites for the green and efficient utilization of coal in China. It is also crucial to achieve high value-added and low-carbon utilization of coal resources. As an important component of coal production and supply in China, approximately 90% of Jurassic coal is classified as low-rank bituminous coal, which is an ideal steam coal and an excellent choice for chemical raw materials. However, the high inertinite content (often exceeding 35%) [1] of Jurassic coal leads to poor coal caking and slurry properties, and degrades the liquefaction and gasification properties of coal [2]. Therefore, effective separation and enrichment of coal macerals is necessary for the green and efficient utilization of Jurassic coal [3].

The methods used for the separation of coal macerals include specific gravity, centrifugation, and flotation [4,5]. Dormans et al. [6] proposed a specific gravity method for separating coal macerals. Based on this method, Dyrkacz and Horwitz [7] further developed the density gradient centrifugal separation technique (DGC), which is currently the commonly used method for separating coal macerals. At the optimal crushing particle size, Men [8] obtained enriched products with a vitrinite content higher than 85% via float-sink tests. Gagarin [9] proposed a distribution function that simulates the separation of coal macerals by density. Ma and Tao [10] reported a better vitrinite recovery of 71.81% using enhanced gravity separation under the optimal experimental conditions. Flotation is a

critical method with prospects for industrial application in the separation and enrichment of coal macerals. Several studies have examined the flotation separation and enrichment of coal macerals via conventional flotation (air flotation), and it was found that vitrinite-rich concentrates can be obtained to a certain extent [11–14]. Despite much progress being made, techniques for separation and enrichment of coal macerals still face several limitations, such as low separation efficiency, low content of separated macerals, and discontinuous separation processes.

Recently, a new method of using oily bubbles as flotation carriers for mineral particles has been gradually adopted by researchers. For example, Liu et al. [15,16] used reactive oily bubbles, i.e., bubbles coated with a thin layer of oil containing a surfactant-modified collector, as flotation carriers for the extraction of oil sands. Wallwork et al. [17] used a collector (oil) flash evaporation device to conduct an oily bubble separation test on difficult-to-float oxidized oil sands, and found that the recovery of oily bubble separation increased by nearly 80%. Yu and Wang [18] took a homemade oily bubble flotation system with hydrocarbon flash evaporation to study the flotation behavior of Shenfu low-rank coal and obtained a low-ash concentrate with a yield higher than 70%. In our previous studies [19–21], it was found that the reactive oily bubble flotation method can significantly reduce reagent consumption and improve the collection ability and flotation selectivity of low-rank bituminous coal. Similarly, Wang et al. [22,23] proved that reactive oily bubbles can indeed improve the quality and flotation performance of low-rank coal. The findings of Zhu et al. [24] indicate that reactive oily bubbles modified by an appropriate concentration and type of surfactant can help improve the flotation efficiency of low-rank coal. Zhou et al. [25–27] reported that oily bubble flotation can effectively improve the flotation recovery of bastnaesite, apatite, dolomite, quartz, and collophane. Ramirez et al. [28] also demonstrated the positive effect of oily bubbles on the flotation recovery of molybdenite under experimental circumstances. Wang et al. [29] also proved that oily bubbles are more hydrophobic than air bubbles, which is conducive to strengthening the bubble–particle attachment and inhibiting the bubble–particle detachment in the flotation column. However, it is still unclear whether oily bubble flotation can promote the flotation performance of coal macerals.

In this work, coal macerals of two Shendong Jurassic coals were enriched using the density gradient centrifugation method. A comparative study of the conventional flotation and oily bubble flotation of the enriched coal macerals was also conducted. The possible mechanism through which oily bubble flotation improves the recovery of coal macerals was explained according to the results of induction time measurements, and wettability and surface group analyses.

2. Materials and Methods

2.1. Sample Preparation

The lump coal used in the test was collected from the 5^{-2} coal seam (designated DLT 5^{-2}) of the Daliuta mine and the 2^{-2} coal seam (BLT2^{-2}) of the Bulianta mine in the Shendong Mining Area, northwest China. The lump was carefully crushed and screened to prepare coal samples with a size less than 0.25 mm for coal maceral enrichment and flotation tests. In this study, centrifugally separated vitrinite-rich coal and inertinite-rich coal were labelled 'V' and 'I', respectively.

The density gradient centrifugation [7] method was used to prepare vitrinite-rich coal and inertinite-rich coal, and the densities of zinc chloride ($ZnCl_2$) specific gravity liquid were set to 1.05, 1.10, 1.15, 1.20, 1.25, 1.30, 1.32, 1.34, 1.36, 1.38, 1.40, 1.42, 1.44, 1.46, 1.48, and 1.50 g/cm^3. The centrifugation speed and time were fixed at 3000 r/min and 25 min, respectively. Figure 1 shows the density distribution of the coal samples. As displayed in Figure 1, the vitrinite-rich of the DLT5^{-2} and BLT2^{-2} coal were concentrated in the density range from 1.30 to 1.38 g/cm^3, and 1.25 to 1.36 g/cm^3, respectively. The inertinite-rich of the DLT5^{-2} and BLT2^{-2} coal were concentrated in the density range from 1.38 to 1.44 g/cm^3.

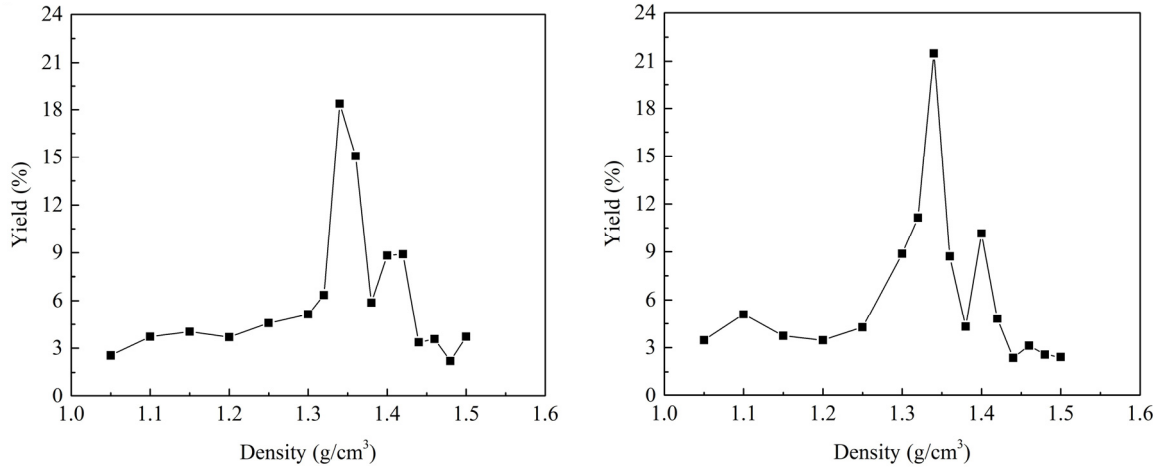

Figure 1. Density distribution of the coal samples: (**a**) DLT5^{-2} coal; (**b**) BLT2^{-2} coal.

Based on the float-sink enrichment results shown in Figure 1, the tail throwing method was adopted to recover the vitrinite-rich coal and inertinite-rich coal, and the enriched centrifuge products were re-enriched. The final enriched products were quantitatively analyzed using a DM4500P type polarization microscope (Leica Microsystems, Germany). The polarization microscope results are presented in Table 1, where the counts are the statistical quantities obtained by the point measurement method. After undergoing two rounds of enrichment, the enrichment rates of the vitrinite-rich and inertinite-rich samples improved significantly, with both exceeding 84%, thereby satisfying the basic requirements for the subsequent single-mineral flotation tests.

Table 1. Results of the enrichment of coal macerals.

Samples	Vitrinite		Inertinite		Mineral		Total
	Counts	Enrichment Rates (%)	Counts	Enrichment Rates (%)	Counts	Enrichment Rates (%)	
DLT5^{-2}-V	834	85.45	127	13.01	15	1.54	976
DLT5^{-2}-I	128	13.20	815	84.02	27	2.78	970
BLT2^{-2}-V	811	85.55	119	12.55	18	1.90	948
BLT2^{-2}-I	122	13.10	788	84.64	21	2.26	931

The proximate analysis of enriched coal macerals consists of the determination of moisture, ash, volatile matter, and fixed carbon contents. Those were determined using a muffle furnace according to the China National Standard (GB/T 212). The ultimate analysis of coal includes the determination of the contents of carbon, hydrogen, nitrogen, sulfur, and oxygen. It was carried out using an elemental analyzer and a sulfur meter according to China National Standards (GB/T 211, 212, 214 and 30733). The proximate and ultimate analysis results of the enriched coal macerals are shown in Table 2, where M, A, V, and FC are the moisture, ash, volatile matter, and fixed carbon contents, respectively (air-dry basis), and C, H, O, N, and S_t are the carbon, hydrogen, oxygen, nitrogen, and total sulfur contents, respectively (dry basis). An examination of the data presented in Table 2 shows that for the DLT5^{-2} and BLT2^{-2} coals, both the C and H contents of the vitrinite-rich component are greater than those of the inertinite-rich coal, while the O content of the vitrinite-rich component is relatively low.

Table 2. Proximate and ultimate analyses of the enriched coal macerals.

Samples	Proximate Analysis, Air-Dry Basis				Ultimate Analysis, Dry Basis				
	M/%	A/%	V/%	FC/%	C/%	H/%	O [1]/%	N/%	S_t/%
DLT5^{-2}-V	7.04	2.40	45.92	44.64	77.10	4.61	16.69	1.15	0.44
DLT5^{-2}-I	6.04	7.52	44.48	41.96	72.90	2.28	22.98	1.28	0.57
BLT2^{-2}-V	6.72	2.48	41.76	49.04	75.44	4.81	17.99	1.29	0.47
BLT2^{-2}-I	7.83	6.16	37.12	48.89	69.67	3.83	25.04	0.91	0.55

[1] O is calculated by the subtraction method.

2.2. Fourier Transform Infrared (FT-IR) Analysis

The surface functional groups of the vitrinite-rich and inertinite-rich materials were analyzed using a Nicolet iS5 Fourier transform infrared spectrometer (FT-IR) manufactured by Thermo Fisher Scientific, Inc. (Waltham, MA, USA). The scanning range was from 4000 cm^{-1} to 400 cm^{-1}, the number of scans was 32, the resolution was 4 cm^{-1}, and the accuracy was less than 0.1 cm^{-1}. The substrate was spectrally pure potassium bromide (KBr). The tablet diameter is 13 mm, and the pressure is 20 MPa. The experimental data were plotted after baseline correction, peak finding, and normalization.

2.3. X-ray Photoelectron Spectroscopy (XPS) Analysis

The surface element contents of the vitrinite-rich and inertinite-rich coal samples were examined using an ESCALAB 250Xi X-ray photoelectron spectrometer (XPS) manufactured by Thermo Fisher Scientific, Inc. (Waltham, MA, USA). The scan data were corrected using a C_{1s} (284.6 eV) internal standard, XPSPEAK 4.1 software was used for peak fitting [19], and the parameter settings [30–34] are given in Table 3.

Table 3. Parameters set for curve fitting in the XPSPEAK software [30–34].

Fitting Range (eV)	Background	L-G	FWHM Range (eV)	C_{1s} Peak Range (eV)	Attribution
(281–295) ± 0.5	Shirley	0	0–2	284.6	C-C/C-H
				285.8–286.3	C-O-C/C-OH
				287.3–287.6	C=O
				289.0–289.2	O=C-O

2.4. Contact Angle Measurements

A JC2000D contact angle measuring instrument was adopted to examine the wettability of the vitrinite-rich and inertinite-rich coal samples by employing the droplet method. The sample was compressed into a tablet under a pressure of 25 MPa for 2 min. The diameter and thickness of the tablet were 13 and 2 mm, respectively. A detailed description of the contact angle measurement process can be found in previous reports [19,35]. In this study, three droplets, namely, water, diesel oil, and modified diesel oil, were taken as the wettability liquids. The average value and the standard deviation from three repeated tests were reported.

2.5. Induction Time Measurements

Induction times between bubbles and coal macerals were measured using a 2017EZ-B+ Induction timer, as shown in Figure 2, manufactured by Oil Sands Environmental Development & Services, Inc. (Edmonton, AB, Canada). For each measurement, coal maceral (0.5 g) was stirred and settled in a beaker containing deionized water, and the suspension was removed. Following this, the coal slurry was transferred to a measurement vessel pre-filled with two-thirds deionized water. This process resulted in the formation of a flat particle bed with uniform thickness at the bottom of the vessel (shown in Figure 3). The amplitude of the bubble motion was set as 3 V, the times to approach and retraction were

fixed on 10 ms, and the air/oily bubble size was kept at 1.3 mm. During the measurement, air needs to be drawn into the glass capillary tube beforehand. When the bottom of the capillary tube was immersed in the water in the measurement vessel through the controller, an air bubble with controllable size could be generated at the end of the capillary tube using a microsyringe. However, it should be noted that when an oily bubble is needed, a small volume of (modified) diesel oil should be sucked into the capillary tube before being immersed in the water. Then, a (modified) diesel oily bubble could be generated at the end of the capillary tube by pushing air using the microsyringe. The generated air/oily bubble was brought into contact with the particle bed for a preset period, as shown in Figure 3. In this way, the corresponding induction time can be obtained. A more detailed description of the measurement process could be found in previous reports [36–38]. The measurements were carried out at room temperature. Each experiment was repeated five times, and the average value was reported.

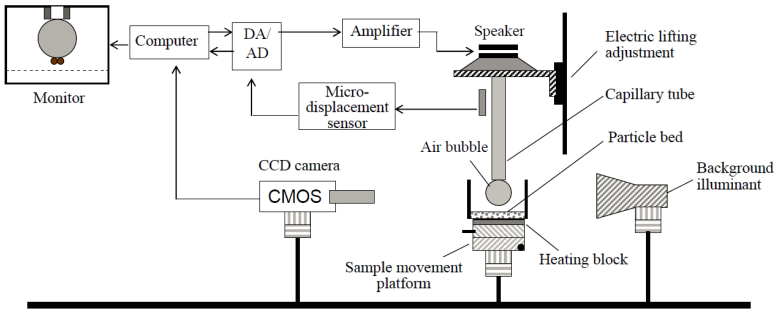

Figure 2. Schematic diagram of induction timer.

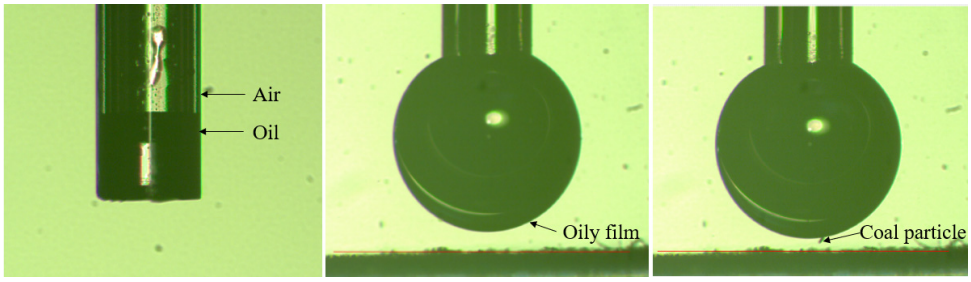

Figure 3. Attachment process of oily bubbles and coal particles.

2.6. Conventional Flotation Tests

For conventional flotation, an XFD-IV flotation machine with a flotation cell volume of 0.5 L was selected. The concentration of the slurry was 40 g/L. The impeller speed and the airflow rate were set at 1996 r/min and 0.02 m^3/min, respectively. Sec-octanol was used as a frother, and the dosage was fixed at 0.90 kg/t. Diesel oil was used as a collector, and the dosages were 0.75, 1.50, 1.98, 2.25, 3.00, 3.75, 4.50, 5.25, and 6.00 kg/t. The skimming time was 3 min. The froth concentrates and the flotation tailings were filtered, dried, weighed and calculated, separately.

2.7. Oily Bubble Flotation and Modification

To obtain a better flotation performance, a custom-made device for oily bubble generation was designed based on the atomization and flash evaporation methods [19]. The schematic diagram of oily bubble flotation setup is shown in Figure 4. According to the characteristics of the test device, the collector (diesel oil) used for oily bubble flotation was added through the inflation tube of the flotation machine at dosages of 0.66, 1.32, 1.98, 2.64, and 3.30 kg/t. The rated air flow rate of atomizer was 6 L/min, and the atomizing rate of collector was kept at 0.299 g/min. The skimming time was 40 s, and the other parameters were the same as those used in the conventional flotation tests. A detailed description of the oily bubble flotation procedure can be found in previous reports [20,36].

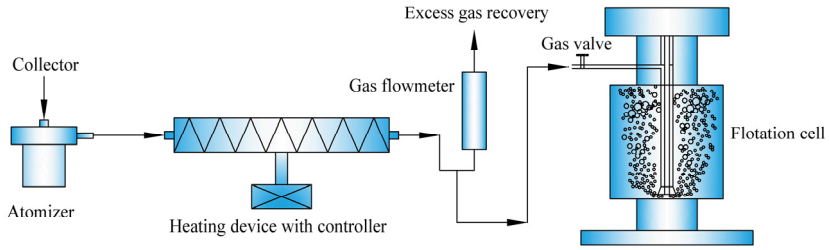

Figure 4. The schematic diagram of oily bubble flotation setup.

Based on the optimal dosage determined from the oily bubble flotation test results (1.98 kg/t diesel oil), diethyl phthalate (DP) was selected as the modifier, and a modified diesel oil was prepared by blending DP and diesel oil at a weight ratio of 2:100. The modified oily bubble flotation processes are the same as those used for oily bubble flotation, except that the diesel oil was replaced with diesel oil modified by DP.

The method for adding and controlling the amount of collector (diesel oil or DP-modified diesel oil) during the flotation experiment was as follows: When the gas valve of the flotation machine was completely closed, the air and collector gasified by heating device would all enter the excess gas recovery device through the gas flowmeter, and the maximum gas flow value (V_0) could be obtained from the gas flowmeter. When the test started, part of the gasified collector and air (V_2) were allowed to flow in the flotation cell for oily bubble flotation, and the remaining collector and air (V_1) would be discharged through the gas flowmeter by adjusting the gas valve of the flotation machine. As a result, the actual required collector and air in the flotation was obtained, i.e., $V_2 = V_0 - V_1$. The atomized collector undergoes rapid expansion upon gasification through the heating device, maintaining a constant mass. It is then uniformly dispersed throughout both the cavity and pipeline. Specifically, the collector drawn from the gas valve of the flotation cell matches the discharge from the gas flowmeter, differing only in volume. During the whole test, sufficient air was sucked in by the atomizer, and there was no air intake in the rest of the process. Therefore, the actual dosage of collector (M_{obf}) in oily bubble flotation could be calculated using Equation (1):

$$M_{obf} = \left(\frac{V_2}{V_0} \cdot M_a \cdot t\right) / m_c \times 1000 = \left(\frac{V_0 - V_1}{V_0} \cdot M_a \cdot t\right) / m_c \times 1000 \quad (1)$$

where M_{obf} is the actual dosage of collector in oily bubble flotation, kg/t; V_0 is the maximum volume of air and collector after atomization and heating flash evaporation, L/min; V_1 and V_2 are the volume of air and collector discharged from the gas flowmeter and sucked into flotation cell, L/min, respectively; M_a is the atomizing rate of collector, which was fixed at 0.299 g/min; t is the oily bubble flotation time, i.e., the skimming time, which was kept at 40 s; m_c is the amount of coal sample used in a single flotation test, which was fixed at 20 g in this study.

In addition, the enriched vitrinite-rich and inertinite-rich coals were approximately treated as pure coal, and their flotation yields were used as the recoveries of concentrate. For both conventional flotation and oily bubble flotation, each experiment was repeated three times, and the average values were reported.

3. Results and Discussion

3.1. Analysis of the Surface Properties of the Coal Samples

3.1.1. Analysis of FT-IR Spectra

Figure 5 shows the FT-IR spectra of the coal samples. It can be seen from the infrared absorption peak characteristic of coal [39–41] observed in Figure 5 that not only hydrophilic oxygen-containing functional groups (-OH, C-O, C=O, etc.) but also hydrophobic -CH_3 and -CH_2 groups, organic sulfur-containing groups (-SH), and some mineral groups (Si-O-Si and/or Si-O-Al, etc.) are present in each coal sample. Functional groups play a vital role in

the adsorption of reagents and determine the surface wettability and floatability of minerals. The contents of hydrophilic oxygen-containing functional groups and hydrophobic groups are discussed in subsequent sections.

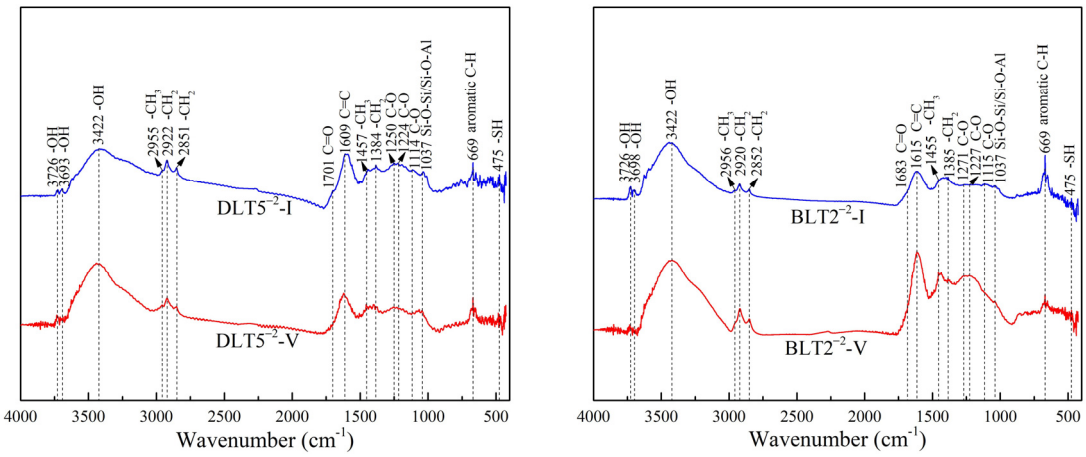

Figure 5. FT-IR spectra of the coal samples: (**a**) DLT5^{-2} coal; (**b**) BLT2^{-2} coal.

3.1.2. XPS Analysis

Table 4 shows the contents of C, N, and O on the surface of the DLT5^{-2} and BLT2^{-2} coals. There are clear differences between the element contents of vitrinite-rich coal and inertinite-rich coal, which match both DLT5^{-2} and BLT2^{-2} well. For DLT5^{-2} coal, the content of C in the vitrinite-rich coal is approximately 2.59% greater than that in the inertinite-rich coal. Conversely, the O and N contents in the vitrinite-rich coal are approximately 2.33% and 0.27% lower than those in the inertinite-rich coal, respectively. For BLT2^{-2} coal, similar experimental results were observed. Clearly, the O/C value of vitrinite-rich coal is lower than that of inertinite-rich coal, which is consistent with the results of proximate and ultimate analyses.

Table 4. The contents of C, N, and O elements on the surface of the DLT5^{-2} and BLT2^{-2} coals.

Element	Element (Atomic) Contents/%			
	DLT5^{-2} Coal		BLT2^{-2} Coal	
	Vitrinite-Rich Coal	Inertinite-Rich Coal	Vitrinite-Rich Coal	Inertinite-Rich Coal
C_{1s}	82.83	80.24	84.18	79.28
O_{1s}	15.22	17.55	14.35	18.40
N_{1s}	1.95	2.22	1.47	2.33
O/C	0.18	0.22	0.17	0.23

Figures 6 and 7 show the C_{1s} fitting spectra of vitrinite-rich and inertinite-rich coal for both the DLT5^{-2} and BLT2^{-2} coal samples. Within the peak range of the functional group containing C, the fitting curves of the vitrinite-rich and inertinite-rich coal samples exhibit a high degree of correspondence with the experimental curves, indicating that the relevant parameters were properly selected and that the fitting process was reliable. Table 5 shows the contents of the C-containing functional groups in the vitrinite-rich and inertinite-rich coal for both the DLT5^{-2} and BLT2^{-2} coal samples. The surface groups of vitrinite-rich and inertinite-rich coal are mainly C-C and C-H, and the oxygen-containing functional groups are mainly hydroxyl (C-OH) and ether groups (C-O-C). In addition, a limited quantity of carboxyl (O-C=O) and carbonyl groups (C=O) are also present. The results show that there are significant differences in the functional groups present in the vitrinite-rich and inertinite-rich coal fractions.

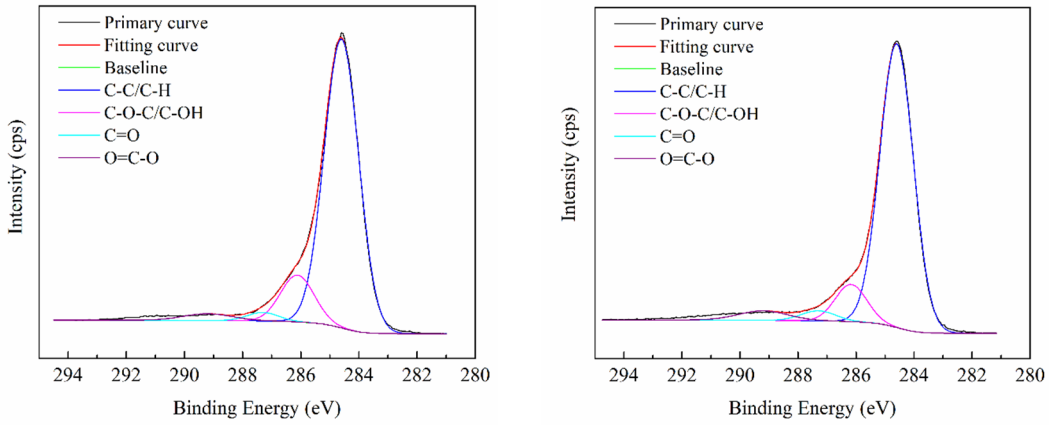

Figure 6. C_{1s} fitting spectra of the DLT5^{-2} coal samples: (**a**) vitrinite-rich coal; (**b**) inertinite-rich coal.

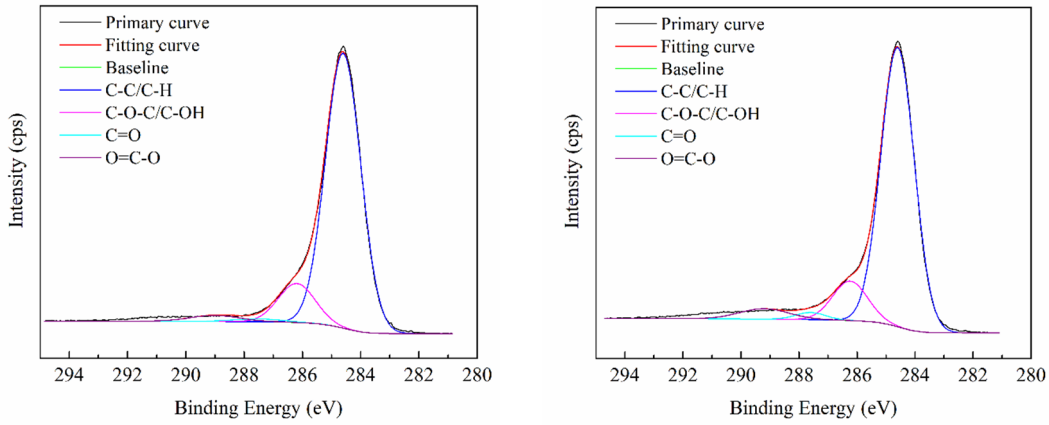

Figure 7. C_{1s} fitting spectra of the BLT2^{-2} coal samples: (**a**) vitrinite-rich coal; (**b**) inertinite-rich coal.

Table 5. C_{1s} fitting data of the DLT5^{-2} and BLT2^{-2} coal macerals.

Functional Groups	Contents in Total Sample/%			
	DLT5^{-2} Coal		BLT2^{-2} Coal	
	Vitrinite-Rich Coal	Inertinite-Rich Coal	Vitrinite-Rich Coal	Inertinite-Rich Coal
C-C/C-H	67.24	60.24	65.82	58.90
C-O-C/C-OH	9.91	8.83	10.37	7.25
C=O	0.22	0.39	0.40	0.66
O=C-O	0.04	0.11	0.05	0.10

For DLT5^{-2} coal, the total content of C-C and C-H groups in vitrinite-rich coal is approximately 7.00% higher than that of inertinite-rich coal, and the total content of hydroxyl (C-OH) and ether groups (C-O-C) in vitrinite-rich coal is only 1.08% higher than that of inertinite-rich coal. However, the content of carboxyl (O-C=O) and carbonyl (C=O) groups in vitrinite-rich coal is approximately 0.24% lower than that of inertinite-rich coal. A similar trend was observed for BLT2^{-2} coal. It can be concluded that the surface of inertinite-rich coal contains more oxygen-containing functional groups and thus is more hydrophilic, reducing its floatability.

3.2. Wettability Analysis

Figure 8 shows the contact angles of water, diesel oil, and DP-modified diesel oil droplets on coal macerals. The contact angle of the water droplets on the surface of the vitrinite-rich coal and inertinite-rich coal of DLT5^{-2} is, respectively, 81.7° and 71.5°, and that for BLT coal is 73.1° and 57.9°, indicating that the vitrinite-rich coal is more hydrophobic, which is highly consistent with the results of the functional group analysis. In addition, for DLT 5^{-2} coal, the contact angle of the diesel oil droplets on the surface of vitrinite-rich coal and inertinite-rich coal is separately 17.9° and 23.7°. Similarly, for BLT2^{-2} coal, the contact angle of the diesel oil droplets on the surface of vitrinite-rich coal and inertinite-rich coal is 19.7° and 26.4°, respectively. The results show that diesel oil droplets can easily spread on the surface of vitrinite-rich coal, which is beneficial for enhancing its hydrophobicity. Moreover, the contact angle of modified diesel oil droplets containing DP on the surface of vitrinite-rich coal and inertinite-rich coal for DLT5^{-2} coal is 16.1° and 18.0°, and that for BLT2^{-2} coal is 16.3° and 18.3°, respectively, indicating that while the addition of DP could further increase the hydrophobicity of both vitrinite-rich coal and inertinite-rich coal, the hydrophobicity of vitrinite-rich coal is still higher than that of inertinite-rich coal.

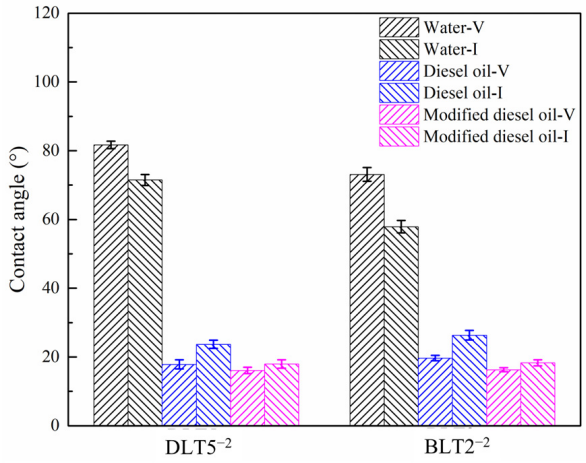

Figure 8. Contact angles of water, diesel oil, and DP-modified diesel oil droplets on coal macerals.

In summary, vitrinite-rich coal exhibits higher hydrophobicity than inertinite-rich coal. Consequently, the (modified) diesel oil droplets easily spread on vitrinite-rich coal, facilitating rapid bubble–particle attachment.

3.3. Induction Times of Air and Oily Bubbles on Coal Macerals

Figure 9 compares the induction times of air, diesel oily, and modified diesel oily bubbles on the surfaces of coal macerals. As shown in Figure 9, the induction time of air (diesel oily or modified diesel oily) bubbles on the surface of vitrinite-rich coal is shorter than that on the surface of inertinite-rich coal. In addition, for both vitrinite-rich and inertinite-rich coal, the induction times of air bubbles on the coal surfaces are greater than 200 ms. However, the induction times of diesel oily bubbles on the surfaces of both vitrinite-rich and inertinite-rich coal are less than 50 ms. Furthermore, for both vitrinite-rich and inertinite-rich coal, the induction times of modified diesel oily bubbles on the surfaces further decrease to less than 45 ms. It could be concluded that the time of adhesion on the coal surface is significantly reduced by the diesel oily bubble, and the addition of DP further reduces the adhesion time between the coal surface and the bubble. Under the same flotation conditions, a shorter induction time may result in rapid collection of the coal macerals during froth production. As a result, higher recoveries of coal macerals could be achieved via (modified) diesel oily bubble flotation due to the shorter induction time. The wettability analysis showed that the modified diesel oil droplet spreads more rapidly than the diesel oil droplet, and both of these spread more rapidly than the water droplet, which consistent with the findings of previous studies [20,22]. Hence, the induction time

results are reliable, and a shorter induction time for vitrinite-rich coal contributes to better flotation performance.

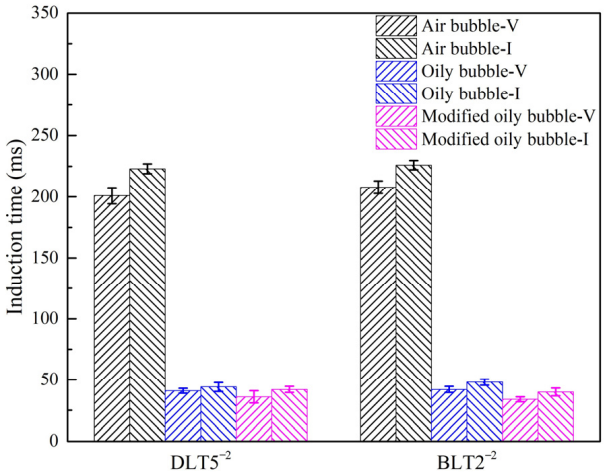

Figure 9. Comparison of the induction times of air, diesel oily and modified diesel oily bubbles on coal macerals.

3.4. Flotation Results of Coal Macerals

3.4.1. Conventional Flotation Tests

Figure 10 shows the results of conventional flotation experiments for DLT5^{-2} and BLT2^{-2} coal macerals. For DLT5^{-2} and BLT2^{-2} coals, the recoveries of vitrinite-rich coal were greater than that of inertinite-rich coal for the same diesel oil dosage. This difference may be ascribed to the higher hydrophobicity of the vitrinite-rich coal, which leads to a shorter induction time of air on the coal macerals and greater flotation recovery. In addition, it was found that when the dosage of diesel oil exceeded 4.50 kg/t, the growth trend of recoveries of vitrinite-rich and inertinite-rich coal disappeared. At a dosage of diesel oil of 6 kg/t, the recoveries of vitrinite-rich and inertinite-rich coal for DLT5^{-2} are approximately 81.58% and 72.82%, and those for BLT2^{-2} are 83.80% and 73.62%, respectively. It is likely that a further increase in the dosage of diesel oil would not enhance the hydrophobicity and reduce the induction time of air on coal macerals. In summary, the higher recoveries of vitrinite-rich and inertinite-rich coal could not be achieved via air bubble flotation.

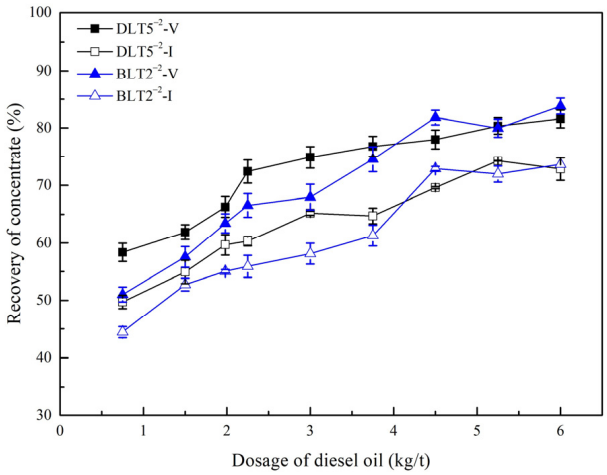

Figure 10. Results of conventional flotation experiments for the DLT5^{-2} and BLT2^{-2} coal macerals.

3.4.2. Oily Bubble Flotation Tests

Figure 11 shows the results of oily bubble flotation of DLT5^{-2} and BLT2^{-2} coal macerals using diesel oil. The results show that the highest recoveries of the coal macerals were at

a collector dosage of 1.98 kg/t. With the present experimental procedure, the aeration rate increased with collector dosage. For collector dosages up to 1.98 kg/t, the air introduced in the flotation cell produced small bubbles. However, above this collector dosage, our observations show that large air bubbles are generated in the flotation cell. Since flotation is an interfacial phenomenon that depends on bubble surface area, the production of large air bubbles results in a decrease in flotation recovery.

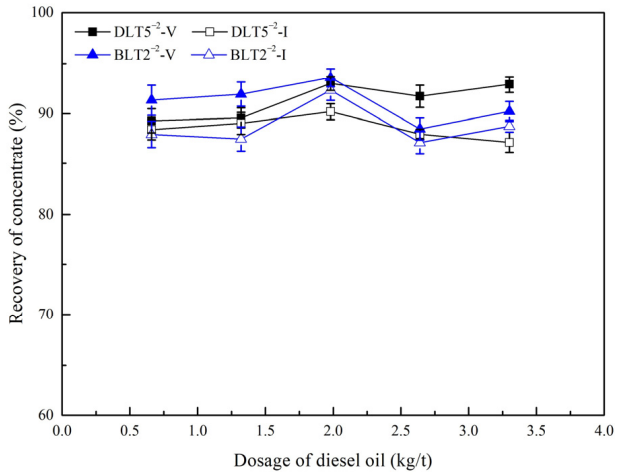

Figure 11. Results of oily bubble flotation of DLT5^{-2} and BLT2^{-2} coal macerals.

Based on the above-described results, the oily bubbles were further modified by the surfactant DP to increase the recovery differences between the vitrinite-rich and inertinite-rich samples for the same coal (DLT or BLT) in order to improve the selectivity of the same collector for the two coal macerals.

The recoveries of conventional flotation and (modified) oily bubble flotation of vitrinite-rich and inertinite-rich coal are compared in Figure 12. Figure 12 shows that the flotation recovery of the vitrinite-rich coal is greater than that of the inertinite-rich coal for both conventional flotation and (modified) oily bubble flotation. At a diesel oil dosage of 1.98 kg/t, the recoveries of vitrinite-rich and inertinite-rich coal of DLT5^{-2} by conventional flotation were 66.27% and 63.43%, and those of BLT2^{-2} were 59.68% and 55.06%, respectively. However, the recoveries of vitrinite-rich and inertinite-rich coal by oily or modified oily bubble flotation were 92.91% and 86.26% for DLT5^{-2}, and that were 90.13% and 82.88% for BLT2^{-2}, respectively. Compared with those of conventional flotation, when oily or modified oily bubble flotation was used, the recoveries of vitrinite-rich and inertinite-rich coal for DLT5^{-2} increased by more than 26.64% and 30.45%, respectively. For modified oily bubble flotation, the recoveries of vitrinite-rich and inertinite-rich coal for BLT2^{-2} were 22.83% and 27.82% higher than those of conventional flotation, respectively. The above results are in agreement with the measurements of the induction times and contact angles between the (modified) diesel oily bubbles and coal macerals. Hence, oily bubble flotation is proven to be an effective method for improving the recoveries of vitrinite-rich coal and inertinite-rich coal.

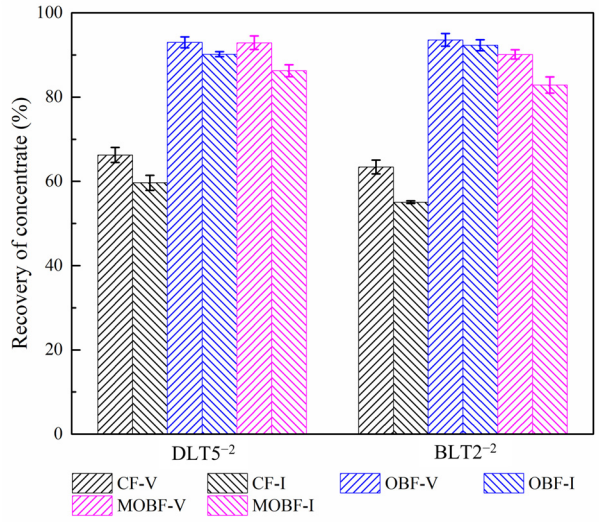

Figure 12. Comparison of conventional flotation and oily bubble flotation of vitrinite-rich and inertinite-rich coal with a diesel dosage of 1.98 kg/t, where CF-V and CF-I represent conventional (air) flotation of vitrinite-rich and inertinite-rich coal, respectively. OBF-V and OBF-I represent oily bubble flotation of vitrinite-rich and inertinite-rich coal, respectively. MOBF-V and MOBF-I represent modified oily bubble flotation of vitrinite-rich and inertinite-rich coal, respectively.

4. Conclusions

In this study, the effect of oily bubbles on the flotation of Shendong Jurassic coal macerals was investigated using FT-IR analysis, XPS analysis, wettability analysis, induction time measurements, and flotation experiments. The following conclusions can be drawn:

1. Enrichment rates exceeding 84% for both vitrinite-rich and inertinite-rich coal can be obtained by the density gradient centrifugation method with two rounds of enrichment.
2. FT-IR and XPS analyses confirmed that there are clear differences in the contents of the C-C, C-H, and oxygen-containing functional groups between vitrinite-rich and inertinite-rich coal, and the O/C value of vitrinite-rich coal is lower than that of inertinite-rich coal.
3. Vitrinite-rich coal has a higher hydrophobicity than inertinite-rich coal, and (modified) diesel oil droplets can further increase the hydrophobicity.
4. The induction time on the coal surface is significantly reduced by diesel oily bubbles, and a further reduction in the induction time between coal macerals and oily bubbles can be obtained by the addition of diethyl phthalate (DP).
5. Oily bubble flotation can significantly improve the recoveries of vitrinite-rich and inertinite-rich coal.

Author Contributions: Investigation, C.L., Q.A., X.L. and H.Z.; Methodology, J.Q. and Z.Z.; Supervision, J.Q., Z.L. and A.Z.; Writing—original draft, J.Q. and Q.A.; Writing—review and editing, J.Q., Z.Z., J.C., S.C. and N.Z. All authors have read and agreed to the published version of the manuscript.

Funding: This work was funded by the National Natural Science Foundation of China (grant number 52004212), the Natural Science Basic Research Program of Shaanxi (grant number 2019JQ-310) and China Postdoctoral Science Foundation (Grant number 2023MD744245).

Data Availability Statement: The data presented in this study are available on request from the corresponding author. The data are not publicly available due to privacy.

Conflicts of Interest: Quan An is an employee of Shaanxi Boxuan Technology Co., Ltd., Xi'an, Shaanxi 710026, China. The paper reflects the views of the scientists and not the company.

Abbreviations

All abbreviations used in this paper are explained as follows:

Abbreviation	Full Name
DLT5^{-2}-V	the vitrinite-rich coal of the 5^{-2} coal seam of Daliuta mine
DLT5^{-2}-I	the inertinite-rich coal of the 5^{-2} coal seam of Daliuta mine
BLT2^{-2}-V	the vitrinite-rich coal of the 2^{-2} coal seam of Bulianta mine
BLT2^{-2}-I	the inertinite-rich coal of the 2^{-2} coal seam of Bulianta mine
M	the moisture content (air-dry basis)
A	the ash content (air-dry basis)
V	the volatile matter content (air-dry basis)
FC	the fixed carbon content (air-dry basis)
C	the carbon content (dry basis)
H	the hydrogen content (dry basis)
O	the oxygen content (dry basis)
N	the nitrogen content (dry basis)
S_t	the total sulfur content (dry basis)
DP	diethyl phthalate
M_{obf}	the actual dosage of collector in oily bubble flotation
V_0	the maximum volume of air and collector after atomization and heating flash evaporation
V_1	the volume of air and collector discharged from the gas flowmeter
V_2	the volume of air and collector sucked into flotation cell
M_a	the atomizing rate of collector
t	the oily bubble flotation time, i.e., the skimming time
m_c	the amount of coal sample used in a single flotation test
CF-V	the conventional (air) flotation of vitrinite-rich coal
CF-I	the conventional (air) flotation of inertinite-rich coal
OBF-V	the oily bubble flotation of vitrinite-rich coal
OBF-I	the oily bubble flotation of inertinite-rich coal
MOBF-V	the modified oily bubble flotation of vitrinite-rich coal
MOBF-I	the modified oily bubble flotation of inertinite-rich coal

References

1. Huang, W.; Tang, S.; Tang, X.; Chen, P.; Zhao, Z.; Wan, H.; Ao, W.; Xiao, X.; Liu, J.; Finkelman, B. The Jurassic coal petrology and the research significance of Northwest China. *Coal Geol. Explor.* **2010**, *38*, 1–6.
2. Chen, P.; Ma, J. Petrographic characteristics of Chinese coals and their application in coal utilization processes. *Fuel* **2002**, *81*, 1389–1395. [CrossRef]
3. Gan, J.; Ma, B.; Shang, J.; Ma, X.; Yang, Z. Formation and development of the coal grading conversion ideas. *Coal Chem. Ind.* **2013**, *41*, 3–6.
4. Zhang, L. Study on Maceral Separation and Characteristics of Maceral Concentrates for Kailuan Coking Coals. Ph.D. Thesis, China University of Mining and Technology (Beijing), Beijing, China, 2015.
5. Honaker, R.Q.; Mohanty, M.K.; Crelling, J.C. Coal maceral separation using column flotation. *Miner. Eng.* **1996**, *9*, 449–464. [CrossRef]
6. Dormans, H.; Hunrjens, F.; van Krevelen, D.W. Chemical structure and properities of coal XX-composition of individual maceral (Vitrinites, Fusinites, Micrinites and Exinites). *Fuel* **1957**, *36*, 321–339.
7. Dyrkacz, G.R.; Horwitz, E.P. Separation of coal macerals. *Fuel* **1982**, *61*, 3–12. [CrossRef]
8. Men, D. Study on the Maceral Crushing and Liberation and on the Coal Blending Coking for Gas Coal. Ph.D. Thesis, China University of Mining and Technology (Beijing), Beijing, China, 2017.
9. Gagarin, S.G. Coal enrichment with separation into fractions by density. *Coke Chem.* **2009**, *52*, 89–93. [CrossRef]
10. Ma, F.; Tao, Y. Study on maceral characteristics and separation of low-rank coal. *Int. J. Coal Prep. Util.* **2023**, *43*, 847–862. [CrossRef]
11. Shu, X.; Wang, Z.; Xu, J. Separation and preparation of macerals in Shenfu coals by flotation. *Fuel* **2002**, *81*, 495–501. [CrossRef]
12. Barraza, J.; Piñeres, J. A pilot-scale flotation column to produce beneficiated coal fractions having high concentration of vitrinite maceral. *Fuel* **2005**, *84*, 1879–1883. [CrossRef]
13. Kopparthi, P.; Singh, R.; Nag, D.; Mukherjee, A.K. Vitrinite maceral separation using column flotation. *Int. J. Coal Prep. Util.* **2018**, *38*, 13–29. [CrossRef]
14. Hower, J.C.; Kuehn, K.W.; Parekh, B.K.; Peters, W.J. Maceral and microlithotype beneficiation in column flotation at the Powell Mountain Coal Mayflower Preparation Plant, Lee County, Virginia. *Fuel Process. Technol.* **2000**, *67*, 23–33. [CrossRef]
15. Liu, J.; Mak, T.; Zhou, Z.; Xu, Z. Fundamental study of reactive oily-bubble flotation. *Miner. Eng.* **2002**, *15*, 667–676. [CrossRef]

16. Xu, Z.; Liu, J.; Zhou, Z. Selective Reactive Oily Bubble Carriers in Flotation Processes and Methods of Generation and Uses Thereof. U.S. Patent No. 6,959,815, 1 November 2005.
17. Wallwork, V.; Xu, Z.; Masliyah, J. Bitumen recovery with oily air bubbles. *Can. J. Chem. Eng.* **2003**, *81*, 993–997. [CrossRef]
18. Yu, W.; Wang, Y. Study on oily bubbles flotation experiment with low rank Shenfu coal. *Coal Sci. Technol.* **2015**, *43*, 152–157.
19. Qu, J. Research on Reactive Oily Bubble Flotation Behavior of Low Rank Coal and Its Flotation Technique. Ph.D. Thesis, China University of Mining and Technology, Xuzhou, China, 2015.
20. Chen, S.; Tang, L.; Tao, X.; He, H.; Yang, Z.; Chen, L. Exploration on the mechanism of oily-bubble flotation of long-flame coal. *Fuel* **2018**, *216*, 427–435. [CrossRef]
21. Chen, S.; Zhou, Y.; Liu, R.; Zhou, A.; Qu, J.; Liu, L.; Zhang, N.; Yu, Y.; Zhu, Z.; Chang, J.; et al. Comparison of attachment process of particles to air and oily bubbles in flotation. *Adv. Powder Technol.* **2023**, *34*, 104059. [CrossRef]
22. Wang, S.; Tao, X. Comparison of flotation performances of low rank coal in air and oily bubble processes. *Powder Technol.* **2017**, *320*, 37–42. [CrossRef]
23. Wang, S.; Liu, K.; Ma, X.; Tao, X. Comparison of flotation performances of low-rank coal with lower ash content using air and oily bubbles. *Powder Technol.* **2020**, *374*, 443–448. [CrossRef]
24. Zhu, C.; Liu, J.; Xing, Y.; Li, M.; Zhang, R.; Li, G.; Gui, X. Investigation of adhesion behavior between reactive oily bubble and low-rank coal. *Colloid Surf. A* **2022**, *632*, 127809. [CrossRef]
25. Zhou, F.; Wang, L.; Xu, Z.; Liu, Q.; Deng, M.; Chi, R. Application of reactive oily bubbles to bastnaesite flotation. *Miner. Eng.* **2014**, *64*, 139–145. [CrossRef]
26. Zhou, F.; Wang, L.; Xu, Z.; Liu, Q.; Chi, R. Reactive oily bubble technology for flotation of apatite, dolomite and quartz. *Int. J. Miner. Process.* **2015**, *134*, 74–81. [CrossRef]
27. Zhou, F.; Wang, L.; Xu, Z.; Ruan, Y.; Chi, R. A study on novel reactive oily bubble technology enhanced collophane flotation. *Int. J. Miner. Process.* **2017**, *169*, 85–90. [CrossRef]
28. Ramirez, A.; Gutierrez, L.; Laskowski, J.S. Use of "oily bubbles" and dispersants in flotation of molybdenite in fresh and seawater. *Miner. Eng.* **2020**, *148*, 106197. [CrossRef]
29. Wang, Y.; Dong, L.; Bu, X.; Ni, C.; Xie, G. Study on inhibition mechanisms of detachment of coal particles from oily bubbles in flotation column. *Powder Technol.* **2024**, *434*, 119368. [CrossRef]
30. Pietrzak, R.; Wachowska, H. The influence of oxidation with HNO_3 on the surface composition of high-sulphur coals: XPS study. *Fuel Process. Technol.* **2006**, *87*, 1021–1029. [CrossRef]
31. Chiang, Y.C.; Lee, C.Y.; Lee, H.C. Surface chemistry of polyacrylonitrile- and rayon-based activated carbon fibers after post-heat treatment. *Mater. Chem. Phys.* **2007**, *101*, 199–210. [CrossRef]
32. Xiang, J.; Hu, S.; Sun, L.; Xu, M.; Li, P.; Su, S.; Sun, X. Evolution of carbon and oxygen functional groups during coal combustion. *J. Chem. Ind. Eng. China* **2006**, *57*, 2180–2184.
33. Kelemen, S.R.; Afeworki, M.; Gorbaty, M.L.; Cohen, A.D. Characterization of organically bound oxygen forms in lignites, peats, and pyrolyzed peats by X-ray photoelectron spectroscopy (XPS) and solid-state ^{13}C NMR methods. *Energy Fuel* **2002**, *16*, 1450–1462. [CrossRef]
34. Perry, D.L.; Grint, A. Application of XPS to coal characterization. *Fuel* **1983**, *62*, 1024–1033. [CrossRef]
35. Zhu, Z.; Zhao, B.; Tian, C.; Sheng, Q.; Li, Z.; Zhang, N.; Wang, J.; Yang, X. Polyaspartic acid, an eco-friendly regulator for the improvement of coking coal flotation: Applications and mechanism. *Int. J. Coal Prep. Util.* **2024**, 1–20. [CrossRef]
36. Chen, S.; Yang, Z.; Chen, L.; Tao, X.; Tang, L.; He, H. Wetting thermodynamics of low rank coal and attachment in flotation. *Fuel* **2017**, *207*, 214–225. [CrossRef]
37. Albijanic, B.; Bradshaw, D.J.; Nguyen, A.V. The relationships between the bubble–particle attachment time, collector dosage and the mineralogy of a copper sulfide ore. *Miner. Eng.* **2012**, *36–38*, 309–313. [CrossRef]
38. Gu, G.; Xu, Z.; Nandakumar, K.; Masliyah, J. Effects of physical environment on induction time of air-bitumen attachment. *Int. J. Miner. Process.* **2003**, *69*, 235–250. [CrossRef]
39. Zou, W.; Cao, Y.; Liu, J.; Li, W.; Liu, C. Wetting process and surface free energy components of two fine liberated middling bituminous coals and their flotation behaviors. *Powder Technol.* **2013**, *246*, 669–676. [CrossRef]
40. Zhu, H.; Li, H.; Ou, Z.; Wang, D.; Lyu, X. Study on surface modification of different rank coals by using FTIR. *J. Chin. Univ. Min. Technol.* **2001**, *30*, 366–370.
41. Wen, S. *Spectral Analysis of Fourier Transform Infrared Spectroscopy*, 2nd ed.; Chemical Industry Press: Beijing, China, 2010.